3rd URSI AT-AP-RASC, Gran Canaria, 29 May – 3 June 2022

Microstrip C patch antenna for hyperthermia treatment: A comparative numerical study with cavity backed C patch antennas

Muthu Rattina Subash Ramu* and Kavitha Arunachalam
Department of Engineering Design, Indian Institute of Technology Madras, Chennai, Tamil Nadu, India

Abstract

In this study, we present the numerical design of a 434 MHz microstrip C patch antenna for hyperthermia treatment. This design is a microstrip realization of our existing water-loaded rectangular cavity backed patch (RCBP) antenna. Electromagnetic (EM) simulation study is carried out on homogenous tissue model to optimize the antenna design parameters. The performance of the optimized antenna is assessed on heterogeneous model derived from breast cancer patient image data. The microstrip antenna has 36 × 36 mm^2 aperture and an integrated 20 mm thick water bolus. The optimized design on homogenous tissue has >90% power coupling with 9 MHz bandwidth (−10dB) and >80% tangential radiated near field. The tissue specific absorption rate (SAR) of the optimized microstrip patch is higher than our existing RBCP antenna with additional advantages of light weight, low profile and fabrication ease. The antenna assessment on patient derived model also indicated >90% power coupling and localized SAR in breast fat and fibro glandular tissues with only 1% SAR in costal cartilage and ribs. It is concluded that the low-profile microstrip C patch could be used for hyperthermia applicator design.

1. Introduction

The most common sites of cancer occurrences in India are the head and neck, and breast, and about 50% are diagnosed at advanced stages [1]. Cancer at advanced stages require adjuvant treatment methods along with the standard treatment procedure. Several clinical trials reported better treatment outcomes when radiation and/or chemotherapy is combined with hyperthermia treatment (HT) i.e., selective heating (40 - 45℃) of cancer tissues for 60 minute duration [2]. Several microwave antennas have been reported for selective heating of cancer tissue. Antennas operating at 434MHz offer better tradeoff between better penetration depth and field size than at higher frequency, and they also meet the frequency band regulations in India. Antennas operating at 434 MHz include the waveguide applicators (Lucite cone [3], box-horn [4]) and microstrip antennas (contact flexible microwave applicator [5], rectangular patch [6] and annular ring [7]). Our earlier works reported the design of water-loaded, circular cavity backed patch antenna [8] which was further miniaturized and modified as rectangular cavity backed patch (RCBP) antenna [9]. The cavity backing provided stable resonance and power coupling in tissues, and suppressed the surface waves, thereby reducing the antenna sensitivity to variations in the tissue load and surroundings.

In this work, we present the microstrip realization of our water-loaded RCBP antenna using a low permittivity low loss substrate. The proposed antenna has the advantages of microstrip patch antennas and is optimized for HT with performance comparable to our existing RBCP antenna.

2. Methodology

2.1 EM simulations

EM simulations were carried out using commercial software (HFSS, Ansys, Canonsburg, PA) which solves for the vector wave equations in frequency domain. The Cole-Cole dielectric model of human breast and body tissues were used in the simulations[10]. In order to reduce computational time and load, optimization of the microstrip C patch was carried out on homogenous tissue model and its performance was assessed on heterogeneous model derived from breast cancer patient image data. The dielectric properties used in the numerical simulations are tabulated in Table 1.The boundaries of the computational domain defined by an air box were assigned as perfectly matched layers to absorb the outward radiated EM fields. Swept frequency simulations were carried out for 1 W excitation fed to the coaxial feed over 425 to 445 MHz .

2.2 Antenna design

Fig. 1 shows the proposed C patch antenna with a coaxial probe feed. The antenna was designed on 1.28 mm thick Rogers RO3010 substrate with lateral dimensions 36 × 36 mm^2. Shorting pins of 0.8 mm diameter separated by 0.2 mm were placed 1 mm from the substrate edges to retain the benefits of cavity backing [8], [9]. The patch design parameters namely, L1 , L2, L3, W and feed location

(x_f, y_f) were determined using parametric sweeps in the numerical simulations to meet the following design objectives: (i) resonance at 434MHz with >90% power coupling to tissue and (ii) convergence of the EM field to single maxima with uniform pattern within the 20 mm waterbolus. The later criteria ensured localized power deposition in the tissue adjacent to the water bolus.

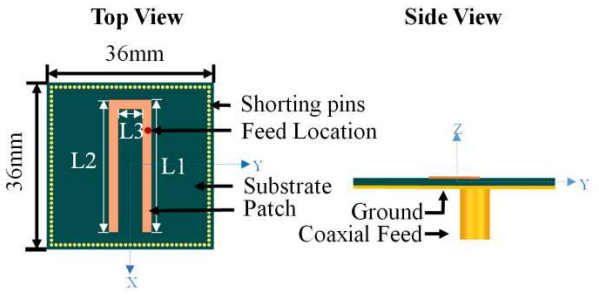

Figure 1. Proposed microstrip C patch antenna design.

2.3 Homogenous tissue model

Fig.2 shows the cut view of the three-dimensional (3D) homogeneous tissue model with the water-coupled microstrip C patch antenna. The 3D model in Fig. 2 was used to optimize the design parameters of the microstrip C patch. The antenna irradiates the homogenous breast tissue (120×120× 80mm^3) through 20 mm thick de-ionized (DI) water contained inside 0.5mm thick silicone rubber. The dielectric properties of the homogeneous tissue is listed in Table 1.

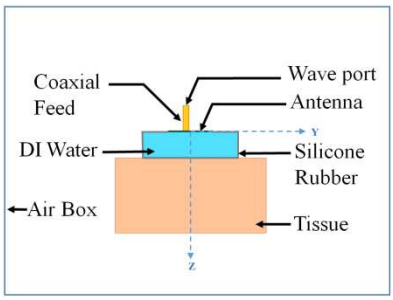

Figure 2. 3D numerical model used for optimization of the microstrip C patch antenna.

2.4 Heterogeneous patient model

The performance of the optimized microstrip C patch antenna was assessed on a randomly selected computed tomography (CT) data of a breast cancer patient downloaded from the cancer imaging archive (TCIA) database[11]. Fig. 3(a) shows the sagittal view of the chosen patient CT data. CT slices inside the rectangular region marked in Fig. 3(a) were segmented using image processing and segmentation algorithms reported in [9] to obtain 3D heterogeneous model containing the body tissues for EM simulations. Fig. 3(b) shows the imported 3D heterogeneous patient model in HFSS with the microstrip C patch antenna and coupling water bolus. Figs. 3(c)-3(d) show the cut views of the 3D patient model imported in HFSS. It can be observed that the patient model is spatially heterogeneous. Due to the body curvature and surface irregularities, small air gaps exist at the interface between the patient model and the silicone rubber bag containing DI water, which mimics the real treatment condition.

Table 1. Material properties at 434 MHz‡

Material domain	Relative permittivity	Conductivity (S/m)
DI water[a]	78.00	0.040
RO3010 substrate[b]	10.20	0.002
Silicone rubber[a]	3.100	0.004
Homogenous muscle	56.00	0.830
Skin	46.40	0.680
Fat	06.00	0.040
Fibro-glandular tissue	53.06	0.840
Cortical bone	13.00	0.090
Lungs (Air)	1.000	0.000

[a]Measured value using DAK TL2 (SPEAG, Zurich, Switzerland),[b]reported in datasheet of Rogers corporation, ‡Tissue properties at 434 MHz [9].

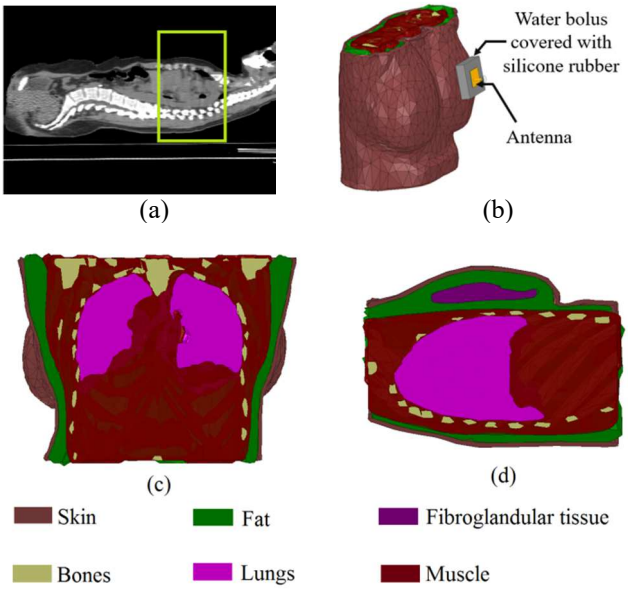

Figure 3. Patient derived heterogeneous 3D model. (a) CT slice indicating the segmented region, (b) Antenna placement on the segmented patient model imported in HFSS, cut views of the 3D patient model in (c) coronal mid plane and (d) para-sagittal plane coinciding with the center of the microstrip C patch antenna.

3. Results and discussion

3.1 Optimized antenna on homogeneous tissue model

The optimized antenna dimensions for 20 mm thick bolus and homogeneous tissue model in Fig. 1 are: $L1$= 28.4mm, $L2$= 5.2 mm, $L3$= 28.4mm, W = 2mm,and feed

location x_f= −7.7mm, and y_f=3.7mm. The power reflection coefficient at 434 MHz and −10 dB bandwidth are−36.3dB and 9MHz, respectively. The normalized SAR in the transverse (XY) and longitudinal (YZ)planes in Figs. 4(a) and4(b), respectively indicate localized power deposition in tissue. The −3 dB SAR coverage of the optimized C patch in the transverse plane calculated at 5 mm depth and penetration depth in the longitudinal plane are 21.92 $cm^2$and 13.20mm, respectively. A comparison of the optimized microstrip C patch with our water-loaded C patch designs inside metallic cavity is summarized in Table 2 [8], [9]. It can be observed that the SAR metrics of the optimized antenna are better than the existing designs. The tangential component of the radiated electric field $\boldsymbol{E}$ at 5mm depth in the tissue is 80% which is lower than our existing designs with 40 mm water bolus. A 40mm water bolus for the optimized microstrip patch improved the tangential component of $\boldsymbol{E}$ in the tissue but at the cost of power loss in the water bolus due to the finite conductivity of the DI water (Table 1).

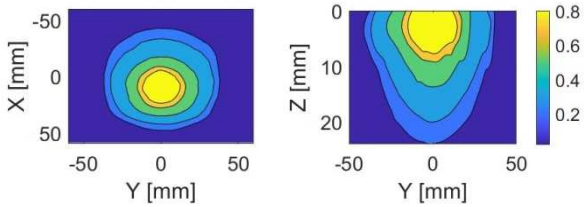

Figure 4. Normalized SAR deposition of the optimized microstrip C patch antenna in homogenous muscle tissue. SAR (a) at 5 mm depth in the transverse plane and (b) longitudinal plane.

Table 2. Comparison of SAR characteristics of the optimized microstrip C patch antenna with existing water-loaded C patch with cavity backing.

Performance	Parameter	[8]	[9]	This work
SAR coverage in XY plane at 5mm depth ($\mathbf{cm^2}$)	–3 dB	18.58	15.03	21.92
SAR penetration depth ($\mathbf{mm}$)	–3 dB	8.87	9.60	13.20
Tangential field at 5mm depth	$\int \frac{\lvert E_x \rvert}{\lvert \boldsymbol{E} \rvert} ds$	89%	82%	80%

3.2 Assessment on patient model

Fig. 5 (a) shows the power reflection coefficient of the optimized microstrip patch antenna for the heterogeneous patient model. It can be observed that the antenna power reflection coefficient for the heterogeneous patient model is comparable with the homogeneous model. Despite the spatial and dielectric heterogeneities of the tissue, and air gaps due to the body curvature and irregularities, antenna power reflection coefficient at 434 MHz is −20.8 dB (>90% power coupling). Figs. 5(b)-(d) show the average SAR (in dB scale) in breast fat, fibro glandular tissue and skeleton for 30 W input power. The peak SAR deposited in the breast fat (at least 11 mm thick) is higher than breast fibro glandular tissue despite the lower electrical conductivity of fat tissue. This is due to the fact that SAR is proportional to $|\boldsymbol{E}|^2$, and electric field $\boldsymbol{E}$ gets attenuated and undergoes multiple reflections as it propagates inside the lossy heterogeneous breast. The following can be concluded from Fig. 5: (i) localized power deposition in breast fat and fibro glandular tissues, (ii) only 1% of the peak SAR is deposited in the skeleton, and (iii) insignificant SAR in heart and lungs, which are organs at risk. These antenna characteristics are desired for HT of superficial breast cancer. The low-profile design can also be adopted for design of phased array applicators for HT [10].

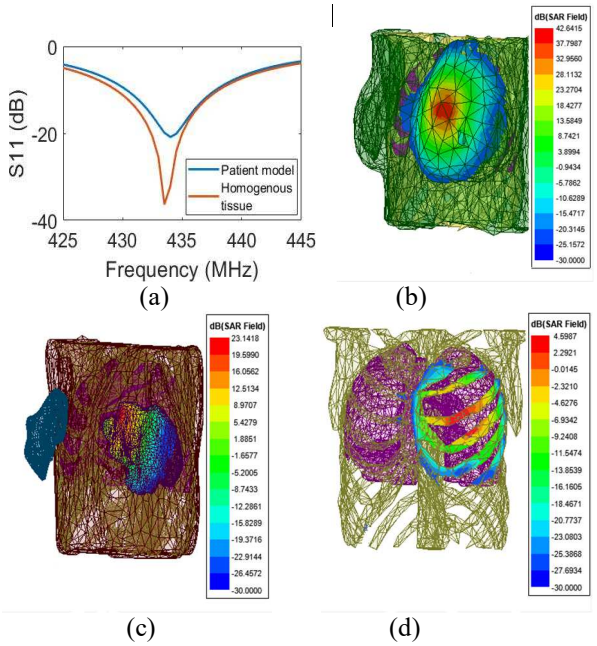

Figure 5. Simulation results of the optimized microstrip C patch antenna for the heterogeneous patient model. (a) power reflection coefficient, tissue SAR in (b) breast fat, (c) breast glandular tissue, and (d) skeleton at 434 MHz .

4. Conclusion

A low profile microstrip C patch antenna was reported for HT of cancer. The antenna design in contact with DI water helped in realizing aperture dimensions comparable to the RCBP antenna. The shorting pins along the periphery of the antenna provided the benefits of the cavity reported in the RBCP antenna design. The 20 mm water bolus thickness for the proposed microstrip C patch reduced the power loss in the coupling DI water and improved tissue SAR. The large field coverage observed at depth is desirable for designing hyperthermia applicator employing an array of the proposed patch antennas. The proposed antenna has better power coupling than the existing cavity backed designs with additional advantages of light weight and low profile. Greater than 90% power coupling and localized SAR observed in the

heterogeneous patient model indicate that the optimized antenna is well suited for hyperthermia applicator design.

References

[1] K. K. Thakur, D. Bordoloi, and A. B. Kunnumakkara, *"Alarming Burden of Triple-Negative Breast Cancer in India,"* (in eng), Clin Breast Cancer, vol. 18, no. 3, June 2018, pp. e393-e399, doi: 10.1016/j.clbc.2017.07.013.

[2] R. D. Issels et al., *"Effect of Neoadjuvant Chemotherapy Plus Regional Hyperthermia on Long-term Outcomes Among Patients With Localized High-Risk Soft Tissue Sarcoma: The EORTC 62961-ESHO 95 Randomized Clinical Trial,"* JAMA Oncology, vol. 4, no. 4, 2018, pp. 483-492, doi: 10.1001/jamaoncol.2017.4996.

[3] G. C. Van Rhoon, P. J. M. Rietveld, and J. Van Der Zee, *"A 433 MHz Lucite Cone waveguide applicator for superficial hyperthermia,"* International Journal of Hyperthermia, vol. 14, no. 1, 1, January 1998, pp. 13-27, doi: 10.3109/02656739809018211.

[4] R. C. Gupta and S. P. Singh, *"Analysis of the SAR distributions in three-layered bio-media in direct contact with a water-loaded modified box-horn applicator,"* IEEE Transactions on Microwave Theory and Techniques, vol. 53, no. 9, 2005, pp. 2665-2671, doi: 10.1109/TMTT.2005.854209.

[5] E. A. Gelvich and V. N. Mazokhin, *"Contact flexible microstrip applicators (CFMA) in a range from microwaves up to short waves,"* IEEE Transactions on Biomedical Engineering, vol. 49, no. 9, 2002, pp. 1015-1023, doi: 10.1109/TBME.2002.802053.

[6] M. M. Paulides, J. F. Bakker, N. Chavannes, and G. C. V. Rhoon, *"A Patch Antenna Design for Application in a Phased-Array Head and Neck Hyperthermia Applicator,"* IEEE Transactions on Biomedical Engineering, vol. 54, no. 11, 2007, pp. 2057-2063, doi: 10.1109/TBME.2007.895111.

[7] S. Curto, P. McEvoy, X. Bao, and M. J. Ammann, *"Compact Patch Antenna for Electromagnetic Interaction With Human Tissue at 434 MHz,"* IEEE Transactions on Antennas and Propagation, vol. 57, no. 9, 2009, pp. 2564-2571, doi: 10.1109/TAP.2009.2027040.

[8] G. Chakaravarthi and K. Arunachalam, *"Design and characterisation of miniaturised cavity-backed patch antenna for microwave hyperthermia,"* International Journal of Hyperthermia, vol. 31, no. 7, 3, October 2015 pp. 737-748, doi: 10.3109/02656736.2015.1068957.

[9] D. Baskaran and K. Arunachalam, *"Design of Site-Specific Microwave Phased Array Hyperthermia Applicators Using 434 MHz Reduced Cavity-Backed Patch Antenna,"* Bioelectromagnetics, https://doi.org/10.1002/bem.22298 vol. 41, no. 8, 1, December 2020, pp. 630-648, doi: https://doi.org/10.1002/bem.22298.

[10] D. Baskaran and K. Arunachalam, *"Design and Experimental Verification of 434 MHz Phased Array Applicator for Hyperthermia Treatment of Locally Advanced Breast Cancer,"* IEEE Transactions on Antennas and Propagation, vol. 69, no. 3, 2021,pp. 1706-1715, doi: 10.1109/TAP.2020.3016462.

[11] K. Clark et al., *"The Cancer Imaging Archive (TCIA): Maintaining and Operating a Public Information Repository,"* Journal of Digital Imaging, vol. 26, no. 6, 12, January 2013, pp. 1045-1057, doi: 10.1007/s10278-013-9622-7.